Collision-system Dependence of the Charge Separation Relative to the Event Plane: Implications for Chiral Magnetic Effect Search in STAR

Niseem Magdy
(For the STAR Collaboration)
Department of Physics
University of Illinois at Chicago
niseem@uic.edu

Outline

- Introduction
- $R_{\Psi_m}(\Delta S)$ Correlator
- $\Delta\,\gamma$ vs $R_{\Psi_m}(\Delta S)$
- Data Analyses
- Results
- Conclusion

❖ Introduction

✓ Chiral Magnetic Effect (CME)

Electric Current

Chiral Magnetic Conductivity

Chiral Chemical potential

$$\vec{J}_Q = \sigma_5 \vec{B}$$

$$\sigma_5 = C_A \mu_5$$

Kharzeev hep-ph/0406125

$$C_A = Q^2 / (4\pi^2)$$

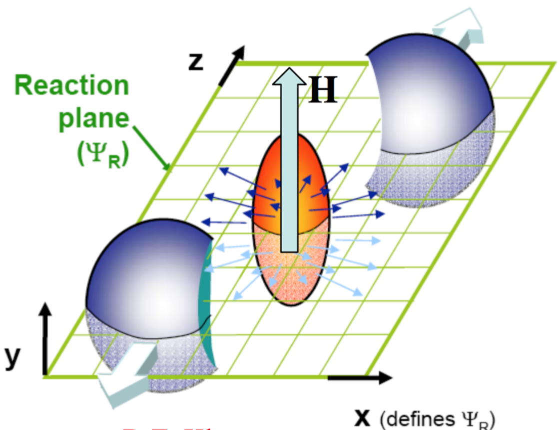

D.E. Kharzeev
Prog.Part.Nucl.Phys. 75 (2014) 133-151

- In non-central collisions, a strong magnetic field is created $\perp$ to Ψ_{RP}

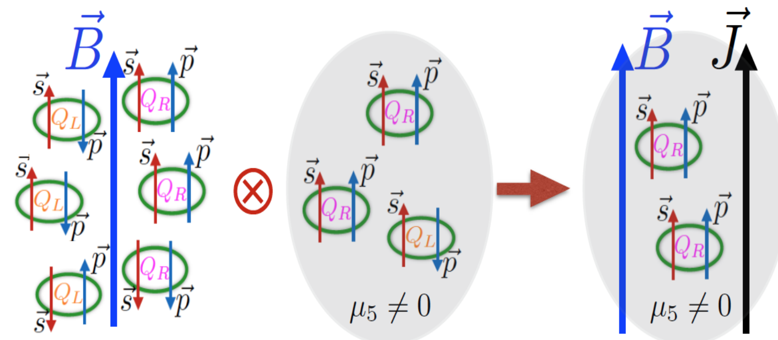

D.E. Kharzeev et al.
Prog.Part.Nucl.Phys. 88 (2016) 1-28

- Magnetic field acts on the chiral fermions with $\mu_5 \neq 0$ leading to an electric current along the magnetic field which leads to a charge separation

❖ Introduction

➢ Chiral Magnetic Effect (CME)

CME-driven charge separation leads to a dipole term in the azimuthal distribution of the produced charged hadrons:

$$\frac{dN^{ch}}{d\phi} \propto 1 \pm 2\, a_1^{ch} \sin(\phi) + \cdots$$

$$a_1^{ch} \propto \mu_5 \vec{B}$$

D.E. Kharzeev
Prog.Part.Nucl.Phys. 75 (2014) 133-151

Strength : eB ~$(m_\pi)^2$ ~10^{18} Gauss

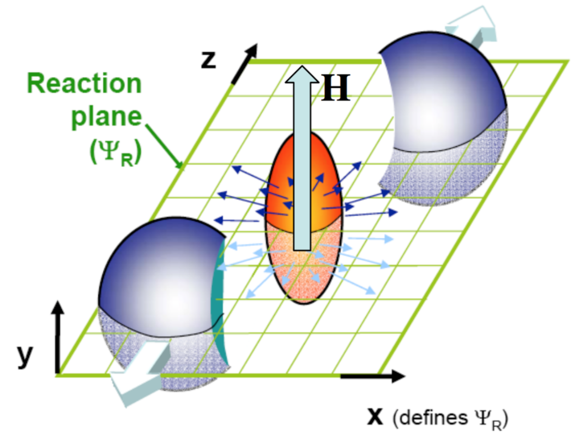

Can we identify & characterize this dipole moment?

➢ What a good correlator should establish?

✓ Leverage Small systems

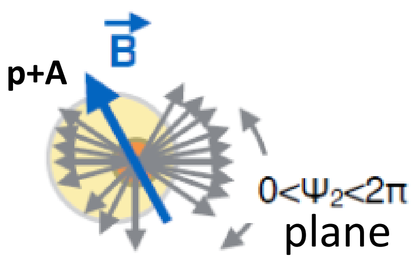

B and Ψ_2 ~ uncorrelated

✓ Leverage Ψ_3 measurements

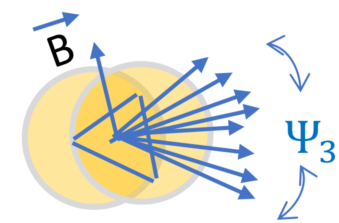

B and Ψ_3 ~ uncorrelated

✓ Excellent benchmark

❖ Introduction

✓ The Gamma correlator

Ma, Zhang
Phys.Lett. B700 (2011) 39-43

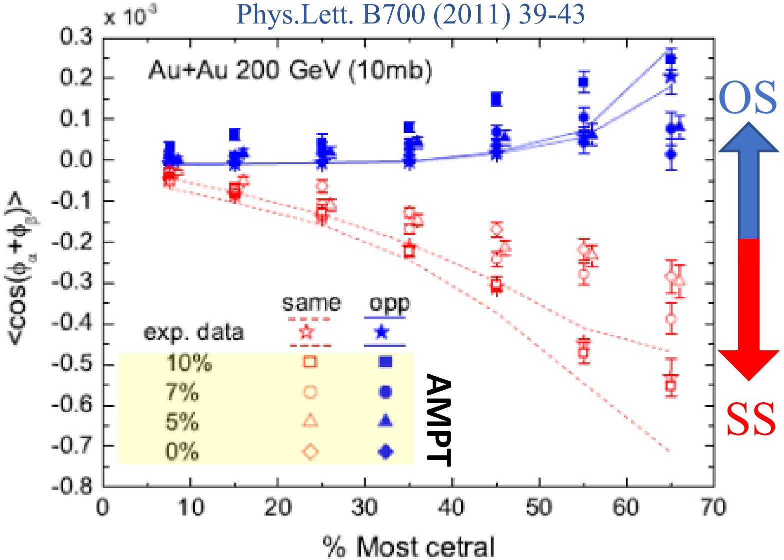

- The Gamma Correlator's response is similar for signal and background
  - ✓ Background-driven correlations complicate CME-driven signal extraction
- Can background account for a part, or all of the observed charge separation signal?

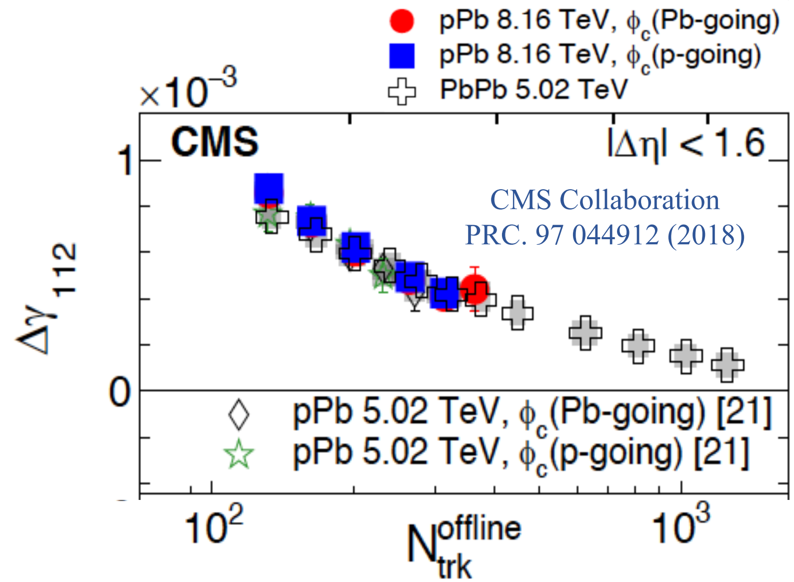

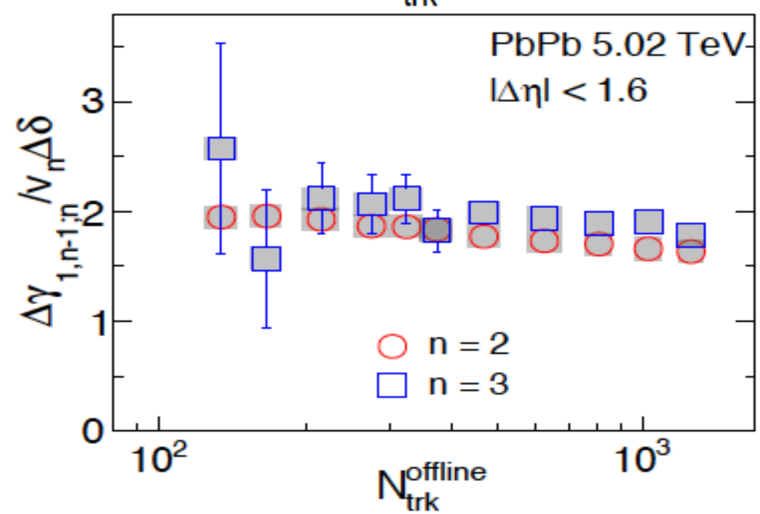

- CMS at QM-18
  - ✓ pPb consistent with 100% BKG
  - ✓ Same for PbPb

❖ $R_{\Psi_m}(\Delta S)$ Correlator

N. Magdy, et al.
PRC 97, 061901 (2018)

➢ The correlator is constructed for a given event plane Ψ_m via a ratio of two correlation functions

$C_{\Psi_2}(\Delta S)$ quantifies charge separation along the B-field

$$R_{\Psi_m}(\Delta S) = \frac{C_{\Psi_m}(\Delta S)}{C^{\perp}_{\Psi_m}(\Delta S)} \;, m = 2 \text{ and } 3$$

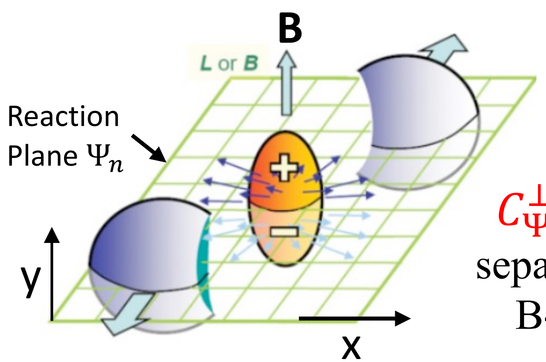

$C^{\perp}_{\Psi_2}(\Delta S)$ quantifies charge separation perpendicular to the B-field (only background)

The $R_{\Psi_2}(\Delta S)$ correlator measures the magnitude of charge separation parallel to the B-field, relative to that for charge separation perpendicular to the B-field

Note that both $C_{\Psi_3}(\Delta S)$ and $C^{\perp}_{\Psi_3}(\Delta S)$ are insensitive to the CME-driven charge separation (only background)

❖ $R_{\Psi m}(\Delta S)$ Correlator

N. Magdy, et al.
PRC 97, 061901 (2018)

$$R_{\Psi m}(\Delta S) = \frac{C_{\Psi m}(\Delta S)}{C^{\perp}_{\Psi m}(\Delta S)}$$

$$C_{\Psi m}(\Delta S) = \frac{N(\Delta S\ \ )}{N(\Delta S_{sh})}$$

$$C^{\perp}_{\Psi m}(\Delta S) = \frac{N(\Delta S^{\perp})}{N(\Delta S^{\perp}_{sh})}$$

$$\Delta\varphi = \varphi - \Psi_{\mathrm{m}}$$

$N(\Delta S)$

$$\langle S^{+}_{\Psi m}\rangle = \frac{\sum_1^p w_p \sin(\frac{m}{2}\ \Delta\varphi)}{\sum_1^p w_p}$$

$$\langle S^{-}_{\Psi m}\rangle = \frac{\sum_1^n w_n \sin(\frac{m}{2}\ \Delta\varphi)}{\sum_1^n w_n}$$

$$\Delta S = \langle S^{+}_{\Psi m}\rangle - \langle S^{-}_{\Psi m}\rangle$$

Sensitive to charge separation
(CME and Background)

w_i: charge dependent detector acceptance.

$N(\Delta S)$

$$\langle S^{+}_{\Psi m}\rangle^{\perp} = \frac{\sum_1^p w_p \cos(\frac{m}{2}\ \Delta\varphi)}{\sum_1^p w_p}$$

$$\langle S^{-}_{\Psi m}\rangle^{\perp} = \frac{\sum_1^n w_n \cos(\frac{m}{2}\ \Delta\varphi)}{\sum_1^n w_n}$$

$$\Delta S^{\perp} = \langle S^{+}_{\Psi m}\rangle^{\perp} - \langle S^{-}_{\Psi m}\rangle^{\perp}$$

$N(\Delta S_{Sh})$

$$\Delta S_{Sh} = \langle S^{+}_{\Psi m}\rangle_{Sh} - \langle S^{-}_{\Psi m}\rangle_{Sh}$$

Shuffling of charges within an event breaks the charge separation sensitivity

$N(\Delta S_{Sh})$

$$\Delta S^{\perp}_{Sh} = \langle S^{+}_{\Psi m}\rangle^{\perp}_{Sh} - \langle S^{-}_{\Psi m}\rangle^{\perp}_{Sh}$$

❖ $R_{\Psi_m}(\Delta S)$ Correlator

➢ Charge separation magnitude is reflected in the width of the $R_{\Psi_m}(\Delta S)$ distribution which is affected by:

✓ Number fluctuations

$\Delta S' = \Delta S/\sigma_{\Delta S^{sh}}$

✓ Empirical EP-resolution

$\Delta S'' = \Delta S'/e^{\left(\left(1-\sqrt{\langle\cos(2\Delta\Psi_2)\rangle}\right)\right)^2}$

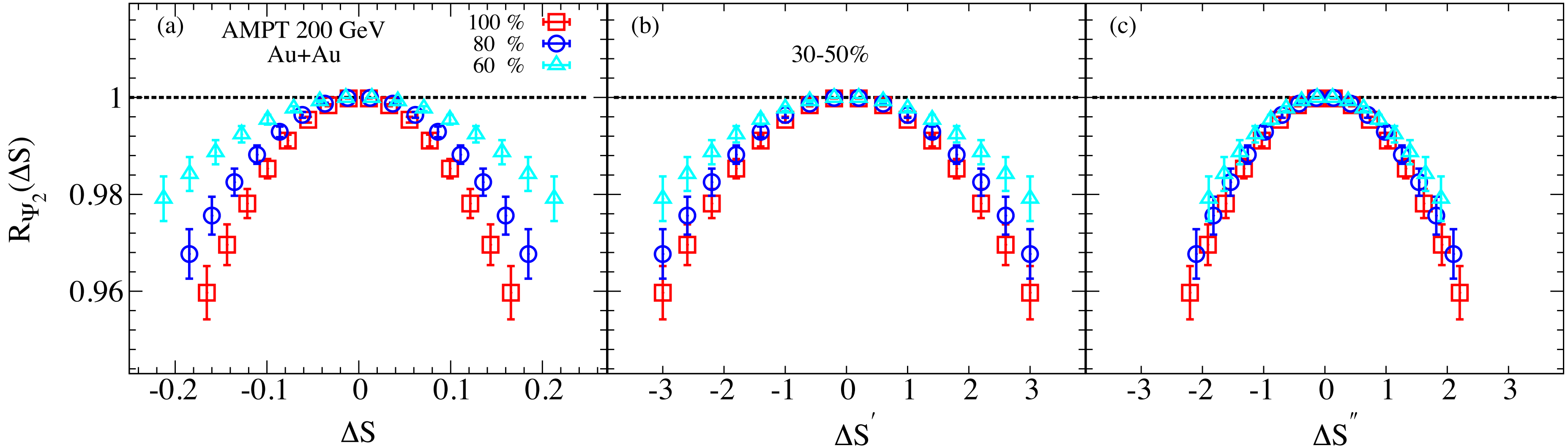

➢ We can account for both number fluctuations and EP-resolution effect on the width of the $R_{\Psi_m}(\Delta S)$

❖ $R_{\Psi_m}(\Delta S)$ Correlator

➢ $R_{\Psi_m}(\Delta S)$ response in background models

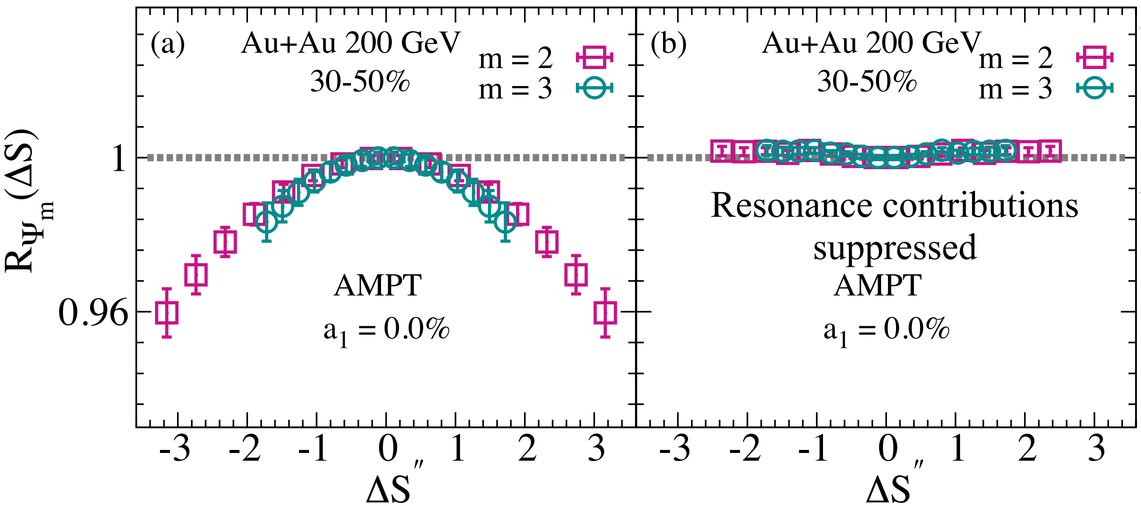

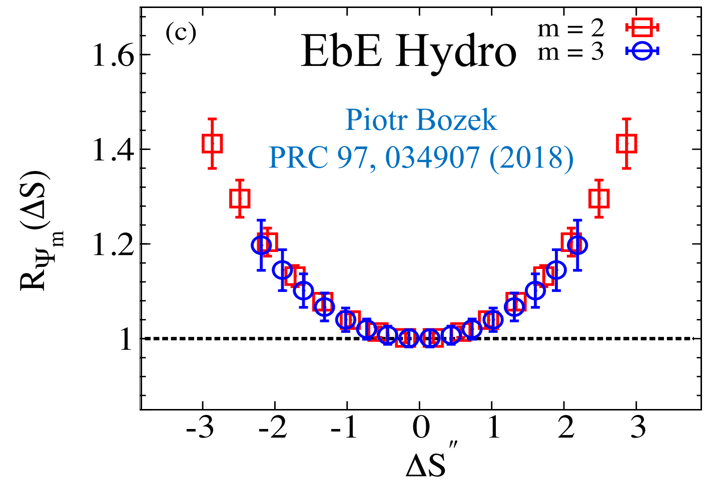

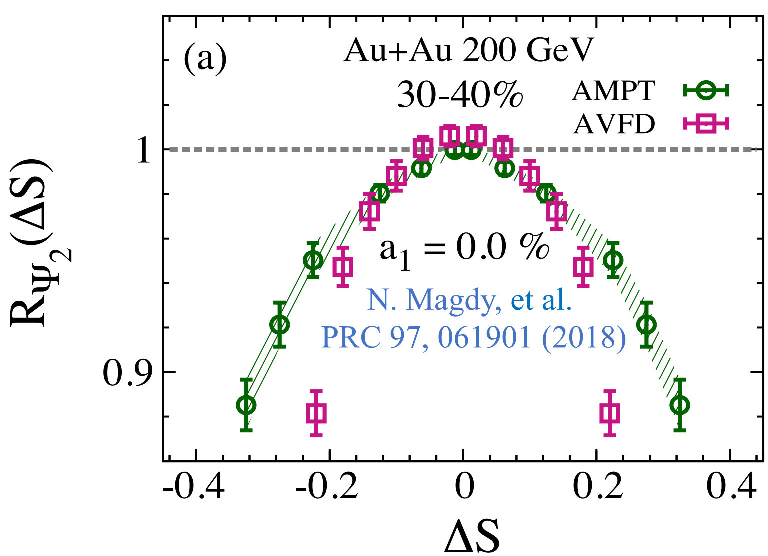

✓ Resonance suppression leads to flat R_{Ψ_m}

✓ The R_{Ψ_2} and R_{Ψ_3} give similar response to the background irrespective of the correlator shape

❖ $R_{\Psi_m}(\Delta S)$ Correlator

➢ $R_{\Psi_m}(\Delta S)$ response in CME models

N. Magdy, et al.
PRC 97, 061901 (2018)

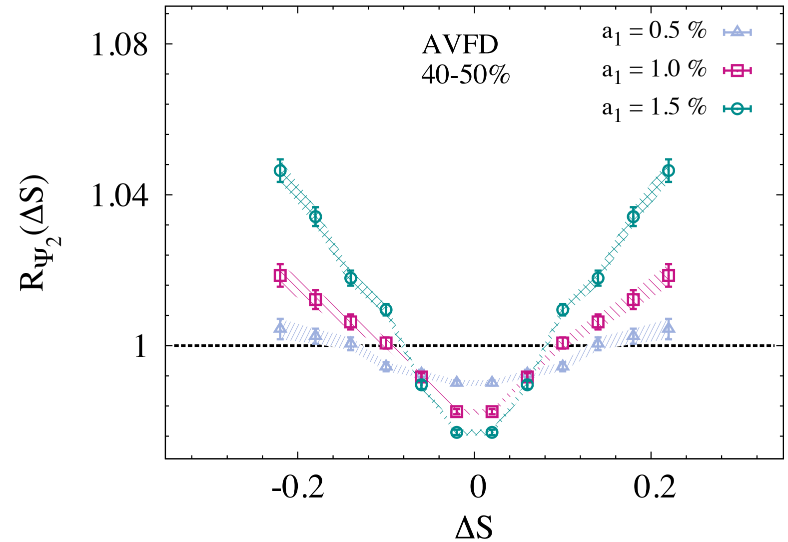

- Signal magnitude is reflected in the widths of the distributions
  - ✓ Smaller widths for larger input signal

- Validation of the expected concave-shaped response of $R_{\Psi_2}(\Delta S)$ to the CME-driven charge separation input in CME-events.

Chiral kinetic approach

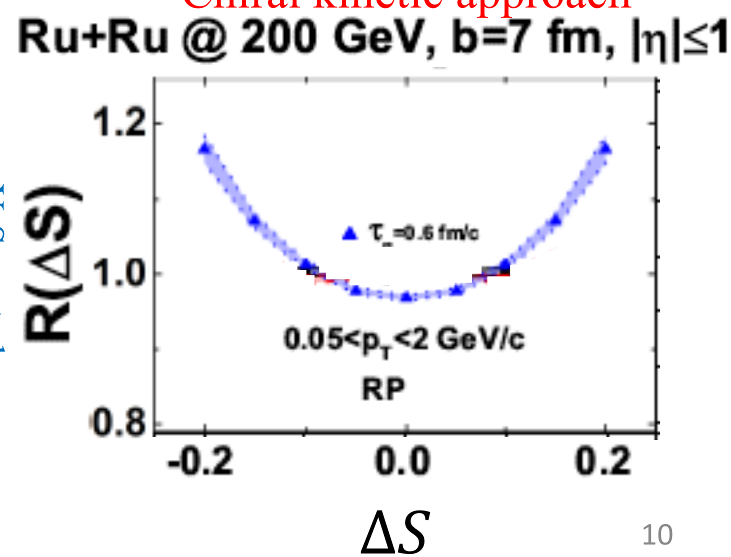

Y. Sun et al.
PRC 98, 014911 (2018)

Concaved-shape distribution for input charge separation

❖ $\Delta\gamma$ vs $R_{\Psi_m}(\Delta S)$

Chiral kinetic approach

Y. Sun et al.
PRC 98, 014911 (2018)

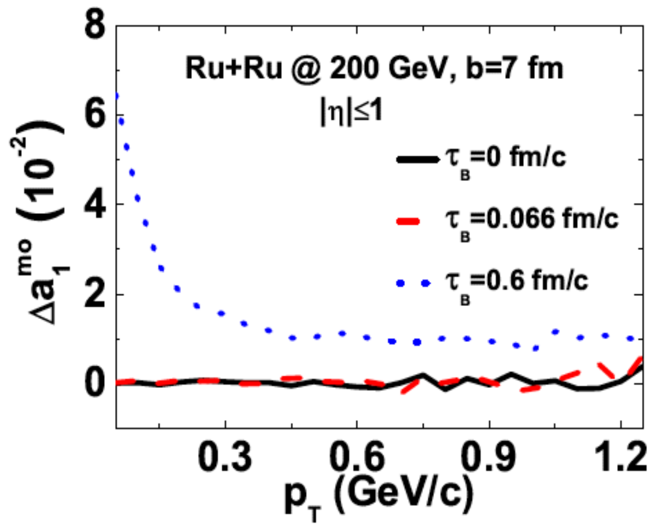

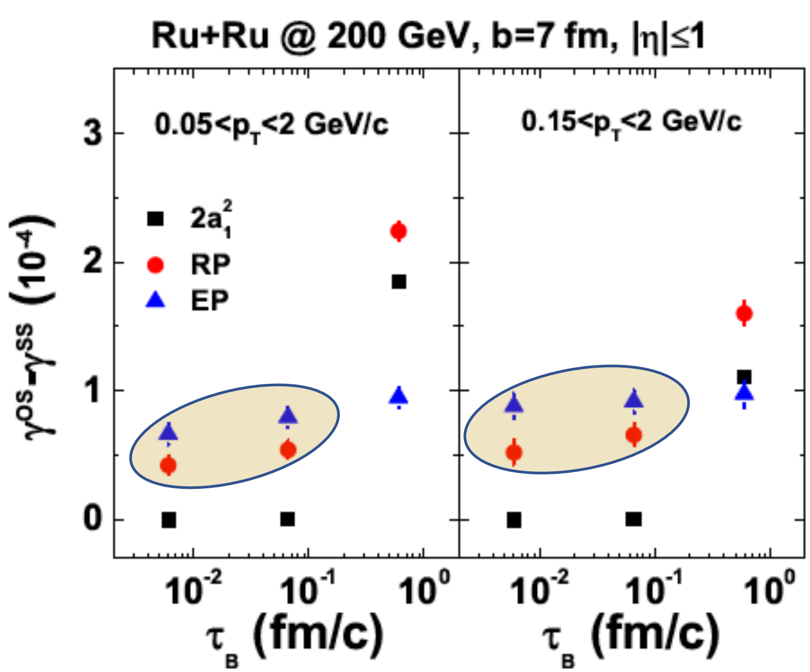

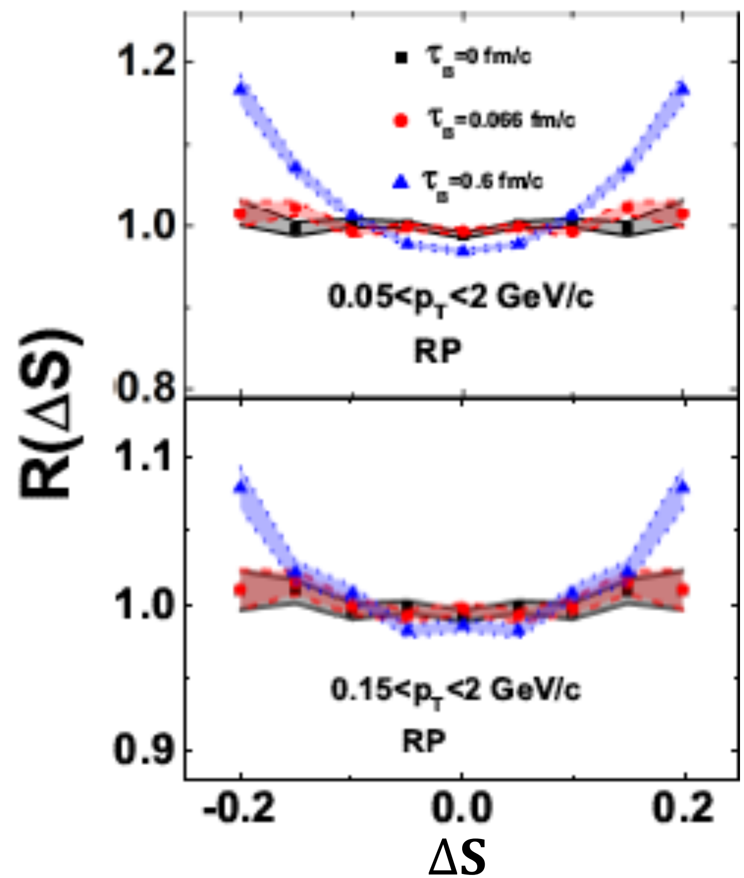

- $a_1 \sim 0$ for $\tau_B < 0.6$ fm/c
  - ✓ $\Delta\gamma$ shows non-zero value
  - ✓ $R_{\Psi_2}(\Delta S)$ shows a flat shape

❖ Data Analysis

The STAR Detector at RHIC

- The TPC detector is used in the current analysis
- Charged hadrons with $0.2 < pT < 2.0$ GeV/c used to construct $\Psi_2^{\eta>0.1}$ & $\Psi_2^{\eta<-0.1}$
- Particles with $0.35 < pT < 2.0$ GeV/c and $\eta < 0$ analyzed using $\Psi_2^{\eta>0.1}$
- Particles with $0.35 < pT < 2.0$ GeV/c and $\eta > 0$ analyzed using $\Psi_2^{\eta<-0.1}$

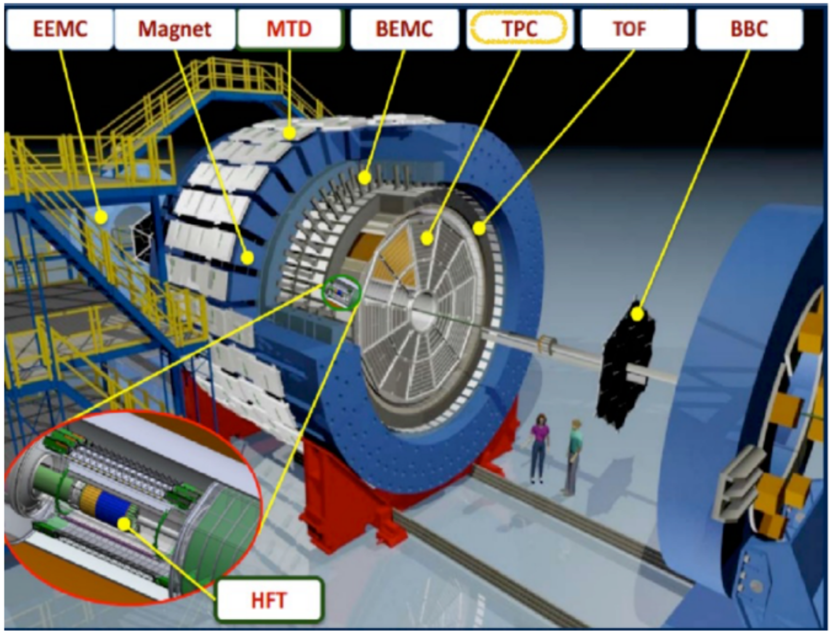

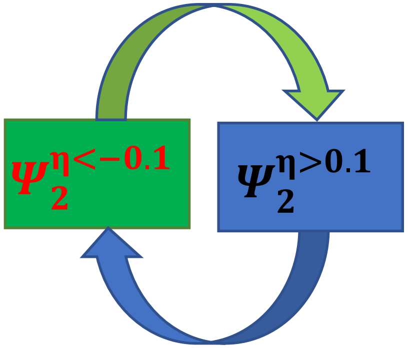

Data Analysis

Event-shape selections (Data)

- ✓ Events are further subdivided into groups with different q_2 magnitude:

$$Q_{2,x} = \sum_{i=1}^{M} \cos(2\,\varphi_i) \qquad Q_{2,y} = \sum_{i=1}^{M} sin(2\,\varphi_i)$$

$$|Q_2| = \sqrt{Q_{2,x}^2 + Q_{2,y}^2} \qquad q_2 = \frac{|Q_2|}{\sqrt{M}}$$

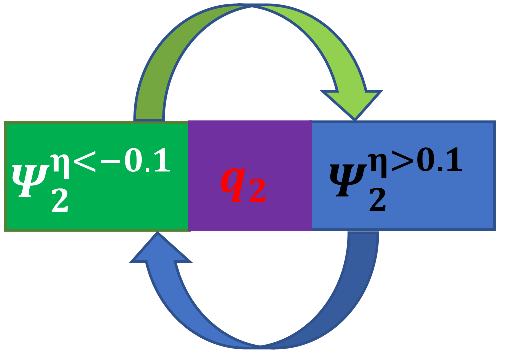

- ✓ The q_2 was created for each N_{ch}

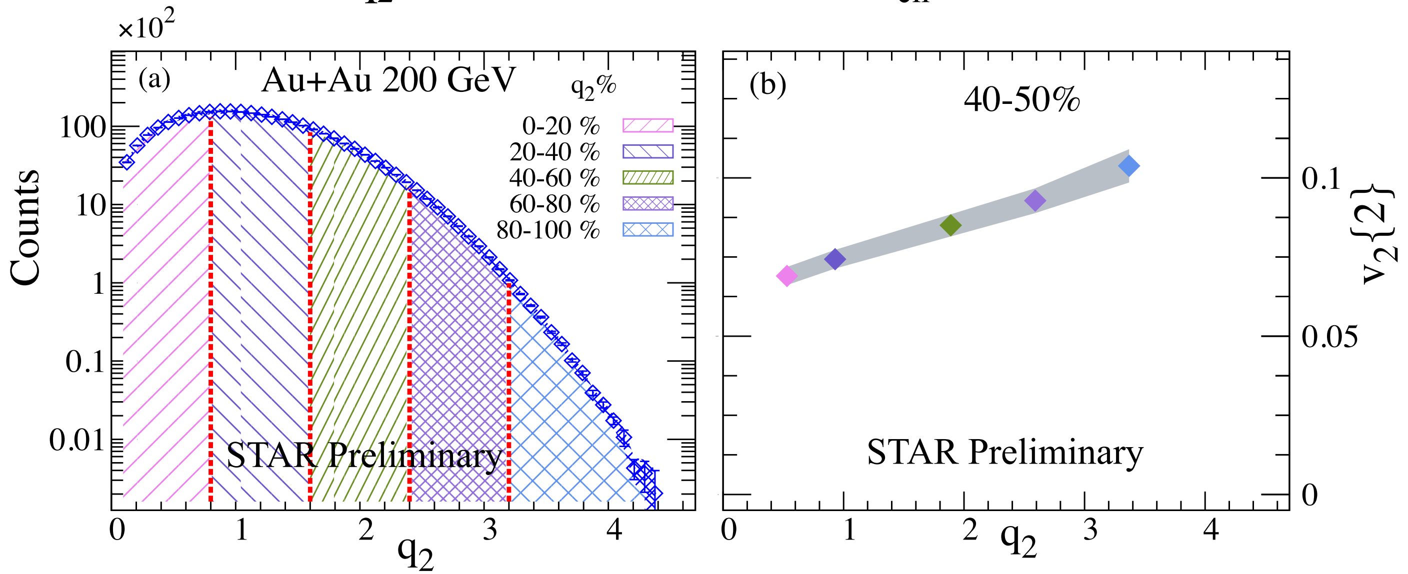

- $v_2\{2\}$ increases linearly with q_2
  - ✓ q_2 is good event-shape selector

Results

❖ Results

- ➢ $R_{\Psi_m}(\Delta S)$ measurements at RHIC
  - ✓ Event plane dependence
  - ✓ Small systems dependence

- ➢ Measurements for R_{Ψ_m} show:
  - ✓ Different response for R_{Ψ_2} and R_{Ψ_3}
  - ✓ Different response for small (p(d)+Au) and large (Au+Au) systems

- ➢ R_{Ψ_m} results are consistent with the expectation for the CME-driven charge separation.
  - ✓ Note that these observations contrast with those from the γ correlator.

[CMS Collaboration arXiv:1610.00263]

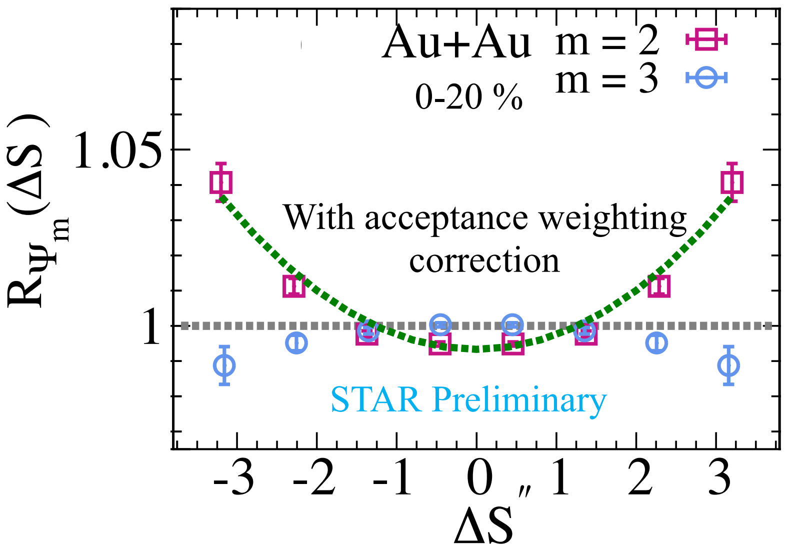

$\frac{Res(p+Au)}{Res(Au+Au)} = 0.45$ $\frac{Res(d+Au)}{Res(Au+Au)} = 0.85$

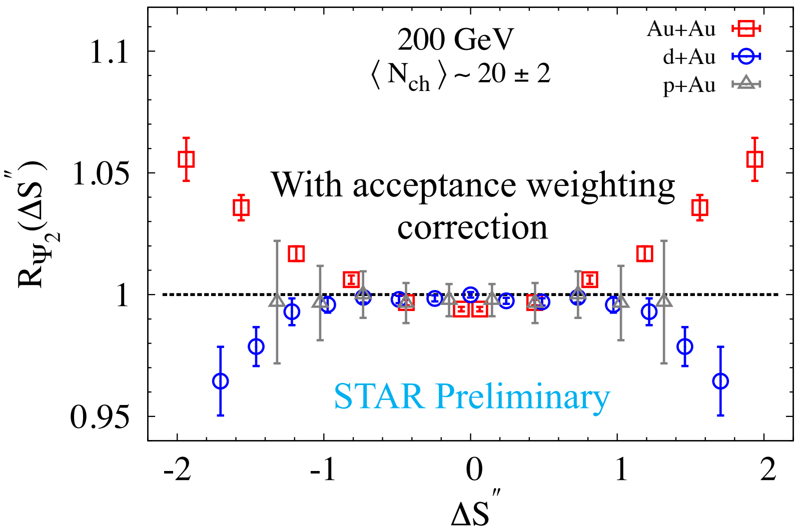

❖ Results

➢ Using acceptance correction (w_i) the charge dependent detector acceptance.

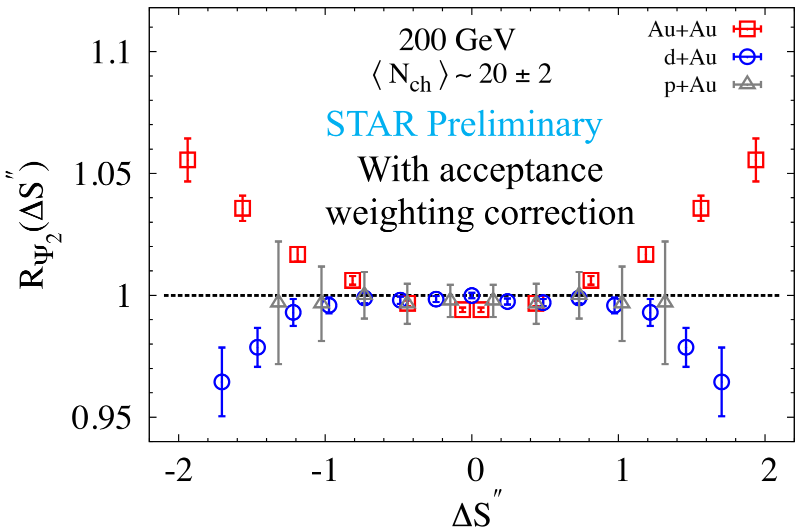

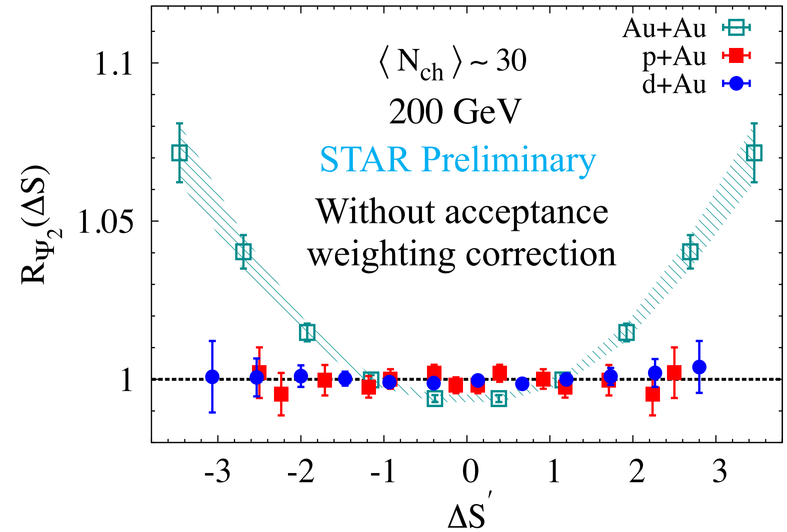

❖ Results

➢ Event shape selection

Comparison of the $R_{\Psi 2}(\Delta S'')$ correlators for q_2 selected events for 30–50% central, Au+Au collisions at 200 GeV for (a) AMPT simulations and (b) experimental measurements.

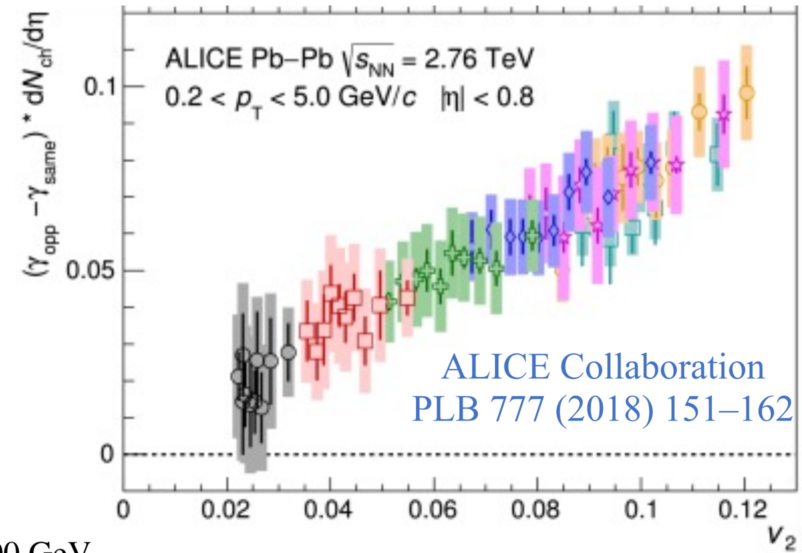

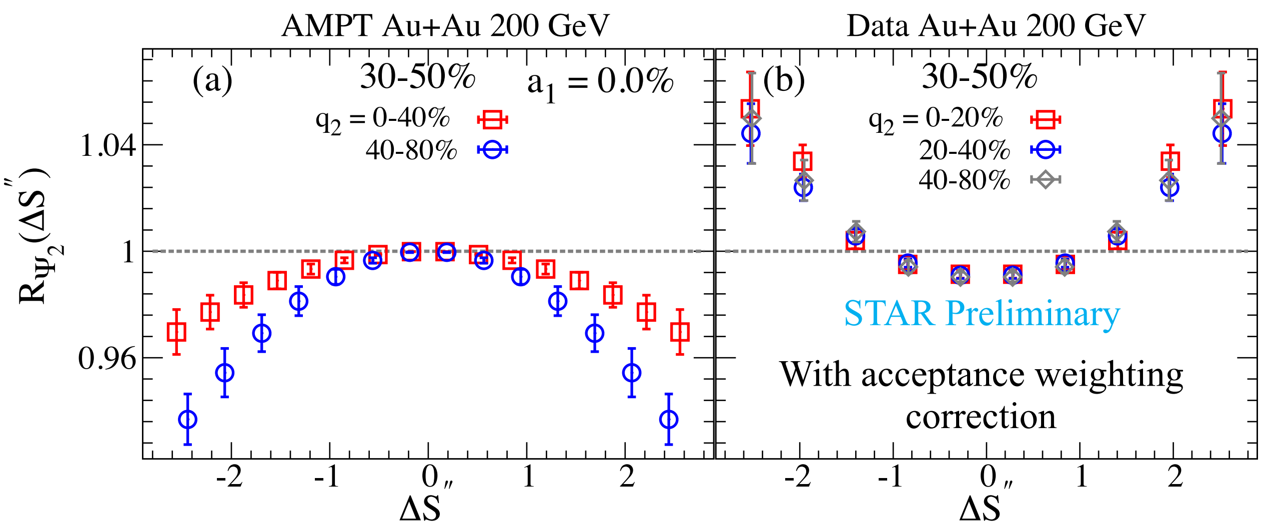

➢ Different q_2 selections (right panel) suggests that $R_{\Psi 2}(\Delta S'')$ is not strongly influenced by the v_2 background-driven charge separation.

❖ Results

➢ Different collision systems $R_{\Psi_2}(\Delta S'')$ and $R_{\Psi_3}(\Delta S'')$

$R_{\Psi_2}(\Delta S'')$ and $R_{\Psi_3}(\Delta S'')$ for 0-20% centrality selection in different collision systems.

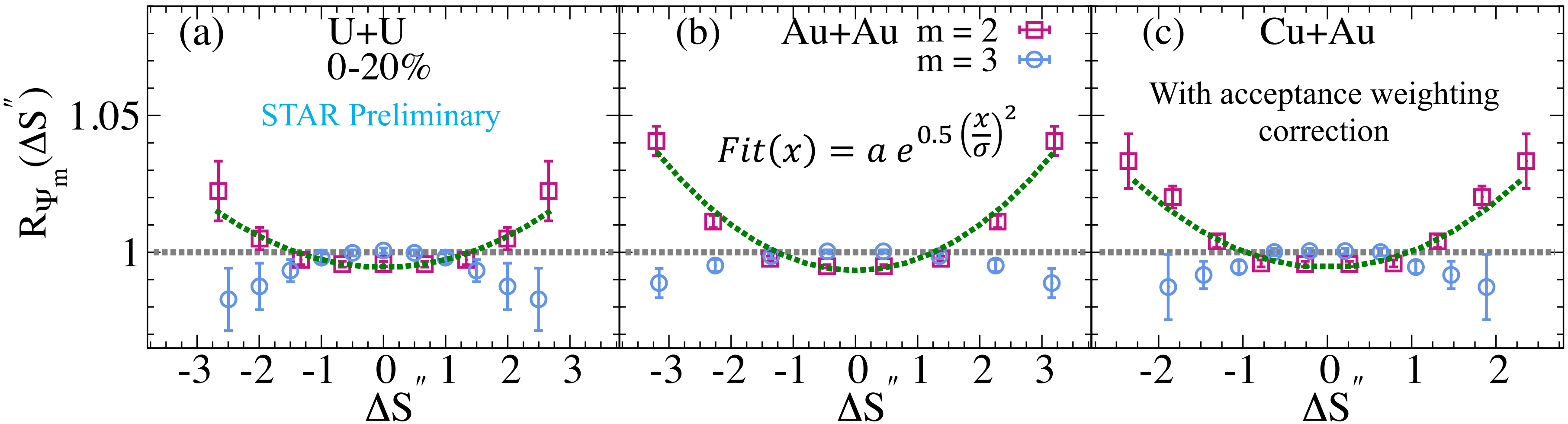

➢ The $R_{\Psi_2}(\Delta S'')$ correlators for different collision systems is strikingly different from those for $R_{\Psi_3}(\Delta S'')$ correlators.

➢ $R_{\Psi_2}(\Delta S'')$ decidedly concave-shaped, as would be expected for CME-driven charge separation with limited influence from background-driven charge separation.

❖ Results

➢ Au+Au collision system $R_{\Psi_2}(\Delta S)$

$R_{\Psi_2}(\Delta S)$ for different centrality selections in Au+Au at 200 GeV.

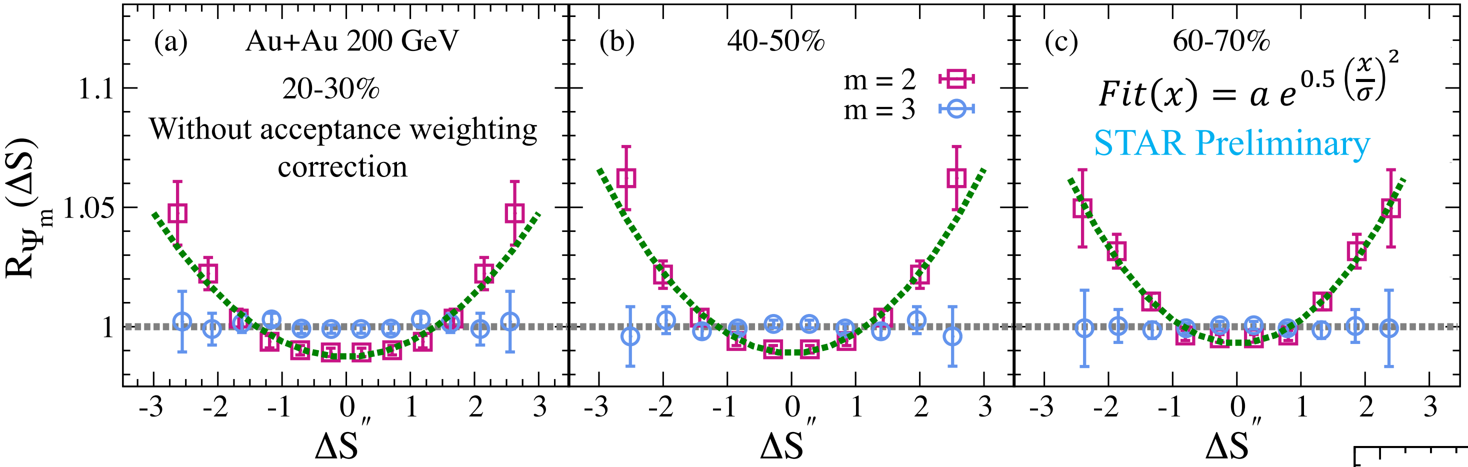

➢ $\sigma^{-1}_{R_{\Psi_2}}$ indicates a sizable centrality dependence, suggestive of the expected increase in the magnitude of the CME-driven charge separation when the $\vec{B}$-field increases as collisions become more peripheral.

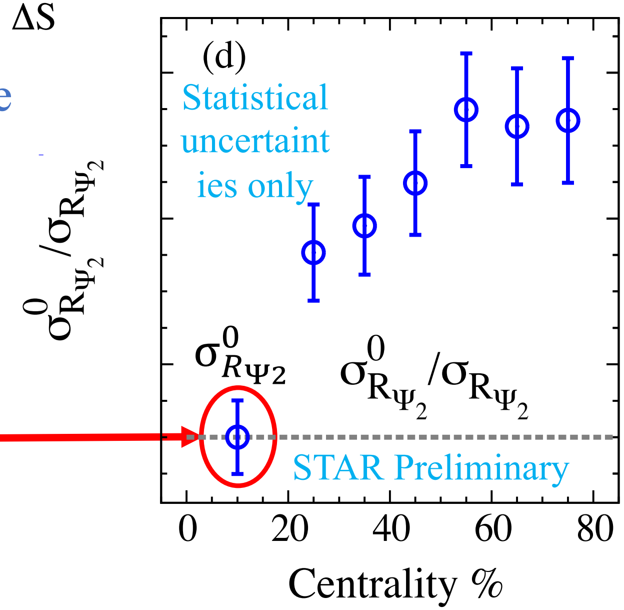

All widths are normalized to the width of 0-20% (smallest a_1)

❖ Results

➢ U+U collision system $R_{\Psi_2}(\Delta S)$

$R_{\Psi_2}(\Delta S)$ for different centrality selections in U+U at 200 GeV.

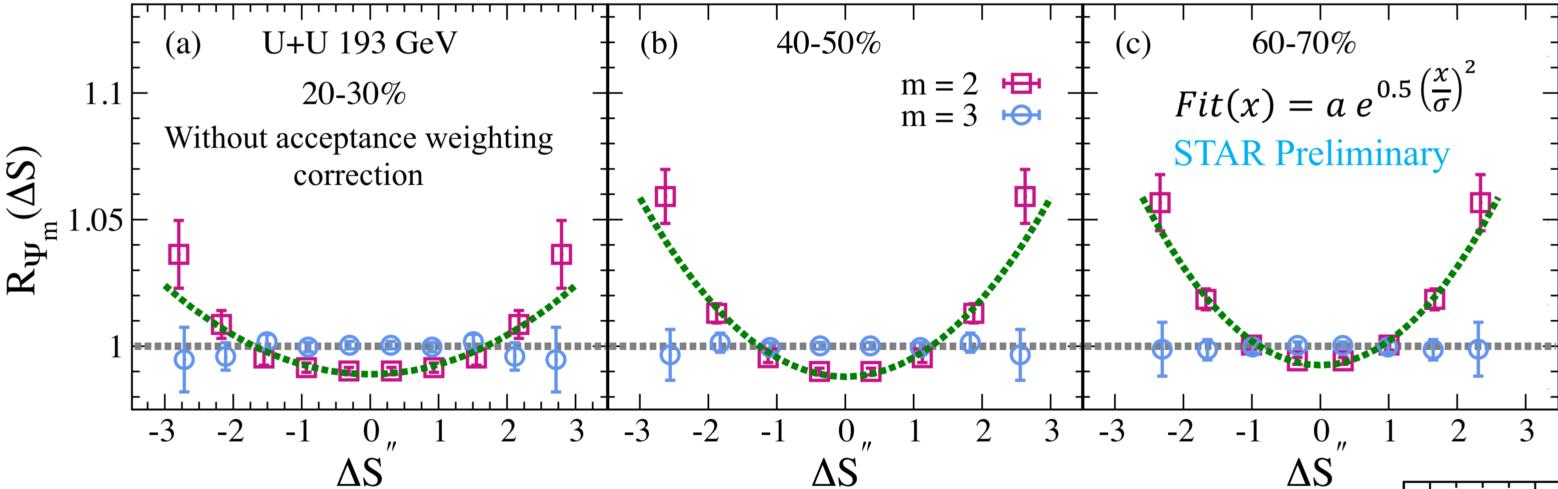

➢ $\sigma^{-1}_{R_{\Psi_2}}$ indicates a sizable centrality dependence, suggestive of the expected increase in the magnitude of the CME-driven charge separation when the $\vec{B}$-field increases as collisions become more peripheral.

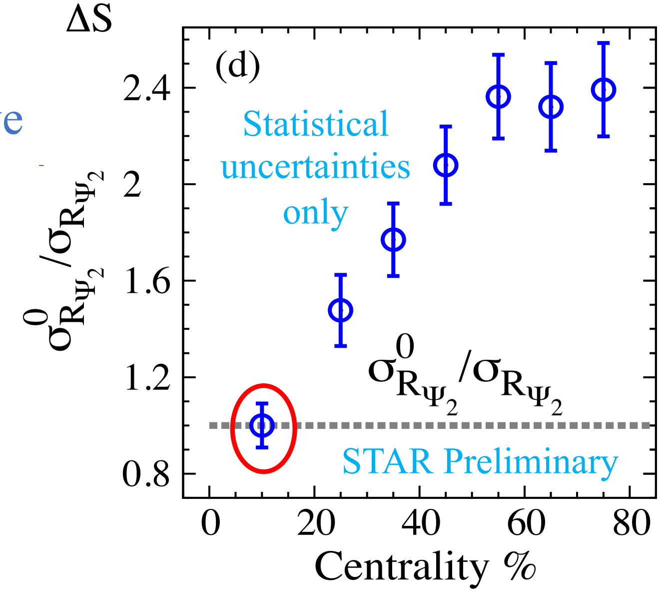

❖ Results

➢ Cu+Au collision system $R_{\Psi_2}(\Delta S)$

$R_{\Psi_2}(\Delta S)$ for different centrality selections in Cu+Au at 200 GeV.

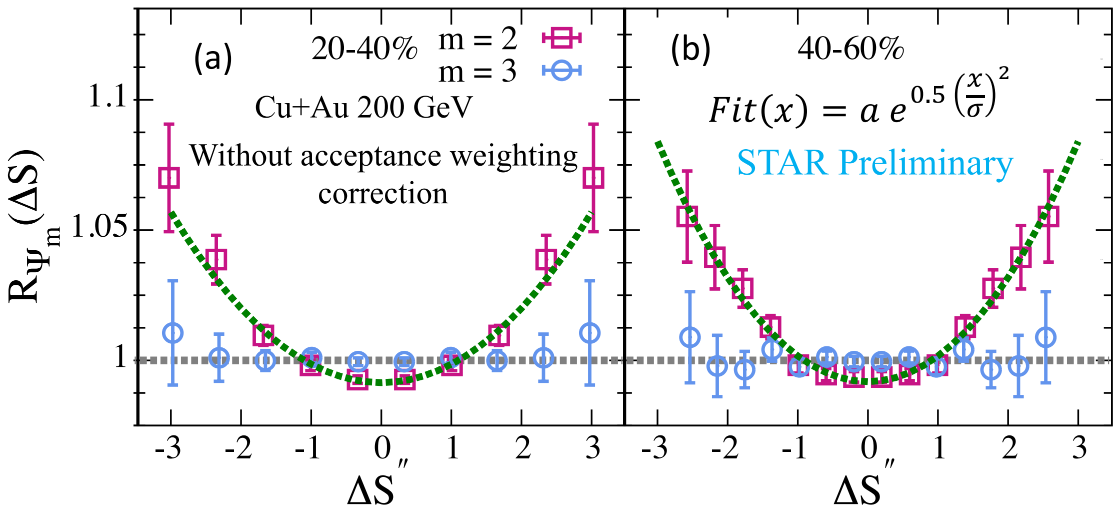

➢ $\sigma^{-1}_{R_{\Psi_2}}$ indicates a sizable centrality dependence, suggestive of the expected increase in the magnitude of the CME-driven charge separation when the $\vec{B}$-field increases as collisions become more peripheral.

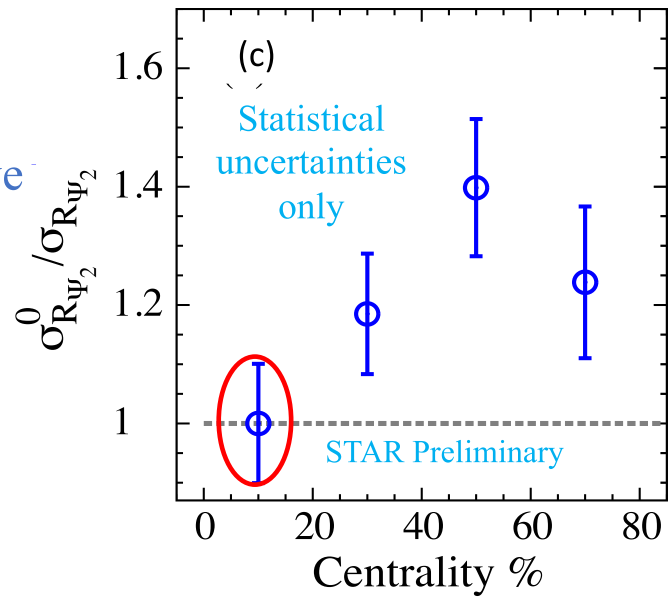

❖ Conclusions

Charge separation measurements performed with R_{Ψ_m}(for m = 2,3) correlator, for U+U (193 GeV), p(d)+Au, Au+Au and Cu+Au at 200 GeV collisions with the STAR detector.

- R_{Ψ_m} measurements show:
  - ✓ Difference in the response for Ψ_2 and Ψ_3 for different collision systems
  - ✓ Difference in the response for small (p(d)+Au) and large systems (Au+Au)

- R_{Ψ_2} width:
  - ✓ Is q_2-independent (weak sensitivity to background)
  - ✓ Is centrality-dependent

- R_{Ψ_m} results are consistent with the expectation for CME-driven charge separation.